Editors' Suggestion

Hydrodynamic permeability of fluctuating porous membranes

Albert Dombret,[1] Adrien Sutter,[1,2] Baptiste Coquinot,[1,3,*] Nikita Kavokine,[2] Benoit Coasne,[4,5] and Lydéric Bocquet[1,†]

[1]*Laboratoire de Physique de l'École Normale Supérieure, ENS, Université PSL, CNRS, Sorbonne Université, Université Paris Cité, 24 rue Lhomond, 75005 Paris, France*

[2]*The Quantum Plumbing Lab (LNQ), École Polytechnique Fédérale de Lausanne (EPFL), Station 6, CH-1015 Lausanne, Switzerland*

[3]*Institute of Science and Technology Austria (ISTA), Am Campus 1, 3400 Klosterneuburg, Austria*

[4]*Université Grenoble Alpes, CNRS, LIPhy, F-38000 Grenoble, France*

[5]*Institut Laue Langevin, F-38042 Grenoble, France*

(Received 27 June 2025; accepted 25 November 2025; published 21 January 2026)

In this paper we examine how porosity fluctuations affect the hydrodynamic permeability of a porous matrix or membrane. We introduce a fluctuating Darcy model, which couples the Navier-Stokes equation to the space- and time-dependent porosity fluctuations via a Darcy friction term. Using a perturbative approach, a Dyson equation for hydrodynamic fluctuations is derived and solved to express the permeability in terms of the matrix fluctuation spectrum. Surprisingly, the model reveals strong modifications of the fluid permeability in fluctuating matrices compared to static ones. Applications to various matrix excitation models, the breathing matrix, phonons, and active forcing, highlight the significant influence of matrix fluctuations on fluid transport, offering insights for optimizing membrane design for separation applications.

DOI: 10.1103/m8h6-1wfk

I. INTRODUCTION

Porous media and membranes are the cornerstone of many industrial processes, from desalination to waste water treatment, from catalysis to energy storage and conversion. Fluid transport through these materials is generally a limiting factor, as the porosity hinders fluid motion. For example, a trade-off is unavoidable in filtration processes between the membrane selectivity (which is promoted by steric sieving) and its permeability (limited by the tortuous viscous flows across the porous matrix [1]). Bypassing such limitations is a key motivation to design new materials and principles for fluid transport [2,3]. Interestingly, nature has found strategies to partly circumvent such limitations, with the paradigmatic example of aquaporins, both selective and highly permeable. Accordingly, the emerging properties of fluid transport at nanoscales, at the heart of nanofluidics, are definitely an asset in this quest [4–6]. A whole cabinet of curiosities has been unveiled, from nearly frictionless flows, dielectric anomalies, memory effects and nonlinear ionic transport, to cite a few [7–9].

Several studies suggested that fluctuations, whether in the fluid or the confining material, are becoming an increasingly significant factor affecting nanoscale fluid transport [10–13]. Wiggling channels were shown to play a significant role in biological transport [14–16], as well as in the diffusion and separation of species across artificial fluctuating channels [17–25], while the flexibility of electrodes materials was shown to accelerate charging dynamics in supercapacitors [26]. It is

*Contact author: Baptiste.Coquinot@ist.ac.at
†Contact author: lyderic.bocquet@ens.fr

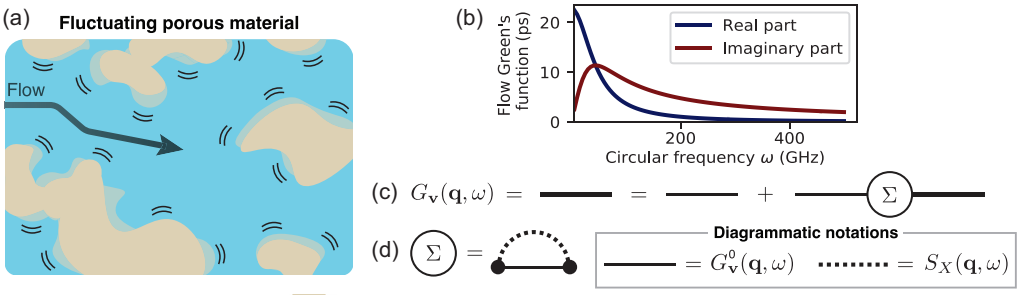

FIG. 1. Model and theoretical procedure. (a) Schematic of the model. We consider a liquid flowing through a fluctuating porous medium. At a coarse-grained level, the dissipation on the matrix is described in terms of a friction-like Darcy term in Navier-Stokes equation, here fluctuating in time and space. (b) Green's function of the flow in absence of thermal fluctuations in the solid as a function of frequency for $q \approx 6\ \mathrm{nm}^{-1}$. (c) Diagrammatic Dyson equation to compute the effective Green's function $G_{\mathbf{v}}$ in the presence of thermal fluctuations of the solid. These fluctuations are taken into account through a self energy Σ. (d) Diagrammatic representation of the self-energy Σ.

also noticeable that transport is not only affected by fluctuations in channel shape, but also by more complex collective modes of the pore walls, such as plasmons, phonons, and so on [27–30]. Hence, this couples nanofluidics with the solid's degrees of freedom at the scale of a single pore [31–33].

In this paper, we investigate theoretically how fluctuations of a porous matrix influence its hydrodynamic permeability. The latter is defined as the averaged fluid velocity $\mathbf{v}_f$ under a pressure gradient ∇P,

$$\langle \mathbf{v}_f \rangle = \frac{\mathcal{K}}{\eta}(-\nabla P), \tag{1}$$

with η the fluid shear viscosity. The permeability has the dimension of a length squared. This is a collective transport property, which can be interpreted, via fluctuation-dissipation theorem, as the collective diffusion of the fluid center of mass [34]. For a static structure, the bare permeability $\mathcal{K}_0$ accounts for the meandering flows across the porous matrix. Now in a fluctuating matrix structure, not only the flow will be affected by the change in the typical pore size, but the breathing of the matrix porosity is expected to induce secondary flows that will impact the global dissipation, hence the permeability $\mathcal{K}$. Molecular dynamics simulations have actually revealed that the impact of wall fluctuations is substantially larger on the collective diffusion as compared to any individual contribution [21]. However, this counterintuitive effect remains so far unexplained.

II. FLUCTUATING DARCY EQUATION FOR THE POROUS FLOW

Fluid transport in porous membranes is usually well described by the coarse-grained Navier-Stokes-Darcy equation [35] and as a minimal model we build on this framework to propose a fluctuating Darcy description to account for the matrix fluctuations

$$\rho_m \frac{\partial \mathbf{v}}{\partial t} = -\nabla P + \eta \Delta \mathbf{v} - \rho_m \xi(X)\mathbf{v} + \delta \mathbf{f}. \tag{2}$$

Here, $\mathbf{v}$ is the fluid velocity, ρ_m its mass density, P the pressure, and $\xi(X)$ the effective friction coefficient of the fluid on the porous matrix according to Darcy's law; X is a (fluctuating) internal parameter characterizing the matrix porosity and its fluctuations. The friction coefficient is *de facto* defined at mesoscales, i.e., scales much larger than the pore sizes, and takes into account the friction encountered by the fluid while crossing the nanopores, see Fig. 1(a). The nonlinear advection term has been discarded since we are interested in low Reynolds-number flows taking into

account fluctuations at frequencies and wave vectors where advection remains negligible. Finally, the fluctuations of the fluid dynamics originate from the Gaussian noise $\delta\mathbf{f}$ whose correlations are linked to the two dissipation terms— the viscosity η and the friction coefficient $\xi(X)$—according to the fluctuation-dissipation theorem.

The space- and time- dependent internal parameter $X(\mathbf{r}, t)$ entering the friction coefficient $\xi(X)$ accounts for the internal microscopic degrees of freedom of the solid matrix and its porosity. For example, below we will assume that X identifies with the normalized fluctuations of the internal density of the breathing solid. In the spirit of [17], we assume that this parameter fluctuates slowly compared to the microscopic processes from which solid-liquid friction emerges—typically above 100 THz for van der Waals and Pauli interactions—but may reach frequencies comparable to hydrodynamic modes. We further assume that its fluctuations are independent from the hydrodynamic fluctuations, which is valid when the modes of the solid either relax quickly to equilibrium or are dominated by an external forcing. Then in its most general form, it is a centered stochastic process characterized by its correlation functions, in particular its structure factor

$$S_X(\mathbf{r}, t) = \langle X(\mathbf{r}, t)X(0, 0)\rangle_0, \tag{3}$$

where the subscript 0 refers to averages taken on the solid matrix fluctuations in the absence of interactions with the fluid.

The equations of motion are complemented by an equation of conservation of mass. In our minimal model, we will restrict to fluctuations of the porous matrix geometry which modify the Darcy friction coefficient $\xi(X)$ but do not involve significant changes of volume, like variations in pore sizes and solid's roughness. As a consequence, the equation of conservation of mass does not involve the variations of X and can be standardly eliminated in Fourier space by applying the projector on transverse modes $\mathbf{J}(\mathbf{q}) = \mathrm{Id} - \mathbf{qq}/q^2$ on the induced velocity field.

Finally, to illustrate the effects of the matrix fluctuations, we will consider a first-order expansion of the friction coefficient in X:

$$\xi(X) = \xi_0 + \xi_1 X(\mathbf{r}, t). \tag{4}$$

Expressions for ξ_1 can be explicited for specific models and can be positive or negative. Beyond this approximation, one could consider higher order in the expansion of $\xi(X)$ in terms of the parameter X. Such corrections will affect the effect of fluctuations on the resulting permeability for strongly fluctuating matrices. We leave such higher-order terms to future work since we are mostly interested in the generic effects of fluctuations on the permeability.

III. FLUCTUATION-INDUCED RENORMALIZATION OF THE PERMEABILITY

A. Quasistatic regime

Let us first consider the limiting regime where the variations of X are much slower than the hydrodynamic fluctuations. The averaged permeability takes the expression $\mathcal{K} = \langle \frac{\nu}{\xi(X)} \rangle$ where the average is taken over X and $\nu = \eta/\rho_m$ the kinematic viscosity. This result should be compared with the "bare" permeability defined in terms of the quasistatic friction coefficient and the average permeability $\mathcal{K}_0 = \frac{\nu}{\langle \xi(X) \rangle}$. Assuming that X follows a Gaussian law, and for the linear model $\xi(X) = \xi_0 + \xi_1 X(\mathbf{r}, t)$, one obtains $\frac{\mathcal{K}}{\mathcal{K}_0} \simeq 1 + (\frac{\xi_1}{\xi_0})^2 \langle X^2 \rangle$,which is valid in the limit of small fluctuations (i.e., neglecting terms beyond $\langle X^2 \rangle$). This quasistatic result is general by convexity and in the quasistatic limit, the average permeability is larger than the permeability obtained from the average friction $\mathcal{K} \geqslant \mathcal{K}_0$. Note that this results remains valid for a quadratic friction model as well, with $\xi(X) = \xi_0 + \xi_1 X(\mathbf{r}, t) + \xi_2 X(\mathbf{r}, t)^2$.

B. General case

In the general case, the fluctuations of X do couple with the hydrodynamic fluctuations described by the fluctuating Darcy equation, Eq. (2), and the quasistatic assumption no longer holds. To calculate the momentum fluctuations and the permeability, one introduces a generic deterministic external force $\rho_m \mathbf{F}_{\text{ext}}(\mathbf{r}, t)$ applied to the fluid in Eq. (2) and computes the resulting velocity field. Going to Fourier space, we thus compute the Green's function $G_{\mathbf{v}}$ of transverse modes of the velocity field—a generalized Stokeslet—such that $\langle \mathbf{v} \rangle = G_{\mathbf{v}} \mathbf{J} \mathbf{F}_{\text{ext}}$, with $\mathbf{J}$ the projector on transverse modes. The permeability $\mathcal{K}$ is then defined as the zero-frequency and zero-wave-vector limit of the Green's function of transverse modes

$$\frac{\mathcal{K}}{\nu} = G_{\mathbf{v}}(\mathbf{q} = 0, \omega = 0). \tag{5}$$

We note that the fluctuation-dissipation theorem allows rewriting Eq. (5) in terms of a Green-Kubo relationship for $\mathcal{K}$, hence interpreted as a collective diffusion coefficient of the fluid center of mass fluctuations.

We now compute the Green's function of the flow in the presence of the fluctuations of the solid. Using Eqs. (2) and (4) and incompressibility, the fluid velocity writes in Fourier space

$$\mathbf{v}(\mathbf{q}, \omega) = G^0_{\mathbf{v}} \mathbf{J}[-\xi_1 X \circledast \mathbf{v} + \delta \mathbf{f} + \mathbf{F}_{\text{ext}}], \tag{6}$$

where $\circledast$ denotes the convolution in both frequencies and wave vectors:

$$[X \circledast \mathbf{v}](\mathbf{q}, \omega) = \int \frac{\mathrm{d}\bar{\mathbf{q}} \mathrm{d}\bar{\omega}}{(2\pi)^4} X(\bar{\mathbf{q}}, \bar{\omega}) \mathbf{v}(\mathbf{q} - \bar{\mathbf{q}}, \omega - \bar{\omega}). \tag{7}$$

Here, we introduce the Green's function of the Darcy equation for a static solid

$$G^0_{\mathbf{v}}(\mathbf{q}, \omega) = \frac{1}{q^2 \nu + \xi_0 - i\omega}. \tag{8}$$

Depending on the wave vector, this noninteracting Green's function, shown in Fig. 1(b), varies typically in the frequency range 10 GHz to 100 THz. If the solid's fluctuations are slow compared to the variations of hydrodynamic velocity, their convolution decouples and we recover the quasistatic limit.

However in the more general case, Eq. (6) should be averaged over the various fluctuations to obtain the effective Green's function of the flow. To this end, we introduce a perturbative expansion of the velocity field $\mathbf{v}$ in the coupling constants ξ_1. At the leading order, we simply have

$$\mathbf{v}_0(\mathbf{q}, \omega) = G^0_{\mathbf{v}} \mathbf{J}[\delta \mathbf{f} + \mathbf{F}_{\text{ext}}], \tag{9}$$

which we then inject in the right-hand side of Eq. (6), providing the basis of a systematic expansion in powers of ξ_1. For instance, we obtain to second order

$$\mathbf{v}_2(\mathbf{q}, \omega) = \xi_1^2 G^0_{\mathbf{v}} \mathbf{J} X \circledast \left\{ G^0_{\mathbf{v}} \mathbf{J} X \circledast \left(G^0_{\mathbf{v}} \mathbf{J}[\delta \mathbf{f} + \mathbf{F}_{\text{ext}}] \right) \right\}. \tag{10}$$

We then average over thermal noise using that $\langle X \rangle = 0$, $\langle \delta \mathbf{f} \rangle = 0$ and $\langle X \delta \mathbf{f} \rangle = 0$. We assume X to be a Gaussian field with correlations

$$\langle X(\mathbf{q}, \omega) X(\bar{\mathbf{q}}, \bar{\omega}) \rangle = (2\pi)^4 \delta(\omega + \bar{\omega}) \delta(\mathbf{q} + \bar{\mathbf{q}}) S_X(\mathbf{q}, \omega). \tag{11}$$

As a consequence, the odd orders of the expansion vanish in average and the first relevant term is

$$\langle \mathbf{v}_2(\mathbf{q}, \omega) \rangle = G^0_{\mathbf{v}} \mathbf{J} \boldsymbol{\Sigma}(\mathbf{q}, \omega) G^0_{\mathbf{v}} \mathbf{J} \mathbf{F}_{\text{ext}}, \tag{12}$$

where we introduce the self-energy

$$\Sigma(\mathbf{q}, \omega) = \xi_1^2 \, [S_X \circledast \alpha_{\mathbf{J}} G^0](\mathbf{q}, \omega). \tag{13}$$

Note that we introduce a factor $\alpha_{\mathbf{J}}$, which is a geometrical factor originating in the projections on transverse modes. As shown in Appendix A, this leads *in fine* to a modification of the prefactor, calculated as 5/6.

Beyond the second order, this expansion can be made systematic thanks to a Dyson equation

$$G_{\mathbf{v}}(\mathbf{q},\omega) = G^0_{\mathbf{v}}(\mathbf{q},\omega) + G^0_{\mathbf{v}}(\mathbf{q},\omega)\Sigma(\mathbf{q},\omega)G_{\mathbf{v}}(\mathbf{q},\omega), \tag{14}$$

which is represented diagrammatically in Figs. 1(c) and 1(d). After resummation, the average fluid velocity then reads $\langle \mathbf{v} \rangle = G_{\mathbf{v}}\mathbf{J}\mathbf{F}_{\text{ext}}$ with an effective Green's function

$$G_{\mathbf{v}}(\mathbf{q},\omega) = \frac{1}{q^2\nu + \xi_0 - \Sigma(\mathbf{q},\omega) - i\omega}. \tag{15}$$

Physically, it corresponds to the Fourier transform of the effective Darcy equation describing the flow after averaging over the fluctuations of the solid.

We can now expand the self-energy Σ in powers of the wave vector $\mathbf{q}$ (there is no linear term in $\mathbf{q}$ due to isotropy), writing

$$\Sigma(\mathbf{q},\omega) = \Sigma(q=0,\omega) + \tfrac{1}{2}\partial_q^2\Sigma(q=0,\omega)q^2 + \cdots, \tag{16}$$

which allows calculating the effective parameters for the Darcy equation in the presence of the matrix fluctuations. At zeroth order, we can interpret the self-energy as a correction to Darcy's friction coefficient. In the present modeling, the apparent friction is always decreased as compared to the static case ξ_0: $\xi_{\text{app}} = \xi_0 - \Delta\xi$, with $\Delta\xi = \Sigma(\mathbf{q}=\mathbf{0},\omega=0) > 0$ calculated as

$$\Delta\xi = \frac{5\xi_1^2}{12\pi^3}\int_0^\infty \mathrm{d}q \int_0^\infty \mathrm{d}\omega\, q^2 S_X(q,\omega)\mathrm{Re}\big[G^0_{\mathbf{v}}(q,\omega)\big]. \tag{17}$$

The renormalized permeability of the system is then deduced as

$$\mathcal{K} = \frac{\nu}{\xi_{\text{app}}} = \frac{\mathcal{K}_0}{1-\frac{\Delta\xi}{\xi_0}}, \tag{18}$$

with $\mathcal{K}_0 = \nu/\xi_0$ the static permeability. Quantitatively, we find that in all practical cases (see below), the permeability cannot be described by the quasistatic result, confirming the need for tackling fluctuations in full generality. We finally note that, similarly to the quasistatic case, non-Gaussian terms have to be accounted for large fluctuations (hence large $\Delta\xi$), which can be handled systematically as additional higher-order self-energy terms. We leave this detailed calculation for future studies and focus here on the qualitative effect of fluctuations on the permeability.

Equations (17) and (18) are the main result of this work. They predict the renormalized permeability in terms of the solid fluctuation spectrum, S_X. Strikingly, under the present assumptions of the model, $\Delta\xi$ is systematically positive and thus the permeability is always enhanced in the presence of fluctuations. Furthermore, according to Eq. (17), the increase in permeability will be maximized when the spectra of the hydrodynamic and solid-state fluctuations do overlap, corresponding to a syntonic frequency matching.

Going now to second order in $\mathbf{q}$ in the expansion of Σ, we find a term that can be interpreted as a correction to the viscosity originating from the coupling of solid correlations to the fluid dynamics. We obtain accordingly an apparent viscosity $\nu_{\text{app}} = \nu + \Delta\nu$, with

$$\Delta\nu = \frac{5\xi_1^2}{6}\int_0^\infty \frac{\mathrm{d}q\mathrm{d}\omega}{4\pi^3}\, q^2 S_X(q,\omega)\partial_q^2\mathrm{Re}\big[G^0_{\mathbf{v}}(q,\omega)\big]. \tag{19}$$

However, in spite of its fundamental interest, we find that this viscosity correction is negligible is most practical situations, see Appendix A.

Altogether, gathering the contributions of the apparent permeability and viscosity, one obtains a renormalized Darcy equation which accounts for fluctuations of the porous matrix. Let us now

apply this formalism to practical situations to evaluate the effects on the permeability. This requires specifying the structure factor S_X of the matrix fluctuations.

IV. APPLICATION TO FLUCTUATING MATRICES

A. Permeability across a breathing array of spheres

As a first, prototypical example, we consider a porous matrix made of an array of fluctuating spheres, with radius R and a number density ρ_s. The liquid can flow through the array, with a Reynolds number assumed to be much lower than 1. In the static case, the permeability $\mathcal{K}$ can be explicitly calculated as a function of the sphere radius R and the volume fraction of the spheres $c = \frac{4}{3}\pi R^3 \rho_s$ [36]. Indeed, the force exerted on the flow by one sphere of the array can be computed as

$$F_1 = 6\pi\eta R\kappa(c)v, \tag{20}$$

where the function $\kappa(c)$ takes the following form for $c \ll 1$:

$$\kappa(c) \simeq 1 + \alpha c^{1/3}, \quad \text{with } \alpha \simeq 1.7601. \tag{21}$$

Then, the volumic friction force that the fluid undergoes when flowing through the medium reads

$$f = \rho_s F_1 = 6\pi\eta\rho_s R\kappa(c)v. \tag{22}$$

Let us now assume that each sphere has some intrinsic *breathing* dynamics, leading to fluctuations of the radius $R = R_0 + r$ of the sphere around a mean value R_0, and that these dynamics are uncorrelated between spheres. One may accordingly define the parameter X for a sphere as the normalized variation of the inner density of the spheres, i.e., $X \equiv (R_0/R)^3 - 1 \simeq -3r/R_0$. The volume fraction c then behaves as $c = c_0(1 + 3r/R_0) = c_0(1 - X)$ Thus, at lowest order in X,

$$f = \rho_m(\xi_0 + \xi_1 X)v, \tag{23}$$

with

$$\xi_0 = \frac{6\pi\eta a\rho_s}{\rho_m}\left(1 + \alpha c_0^{1/3}\right) \quad \text{and} \quad \xi_1 = -\frac{2\pi\eta a\rho_s}{\rho_m}\left(1 + 2\alpha c_0^{1/3}\right). \tag{24}$$

We now specify the breathing dynamics for r, which we model by an overdamped Langevin equation on r. We denote by ω_0 the intrinsic breathing frequency of the sphere, and γ the damping rate of the *breathing* modes, such that the fluctuating dynamics of the sphere reads

$$\gamma\dot{r} = -\omega_0^2 r + \frac{1}{m}\delta f(t), \tag{25}$$

with m an apparent mass of the radius dynamics and $\delta f(t)$ being some Gaussian noise with zero average. We can then directly compute the fluctuations of the sphere radius, embedded in its structure factor $S_r(t - t') = \langle r(t)r(t')\rangle$. The Fourier transform of S_r is found by either solving the Langevin equation or using the fluctuation-dissipation theorem

$$S_r(\omega) = \frac{2\gamma k_B T}{m}\frac{1}{(\gamma\omega)^2 + \omega_0^4}. \tag{26}$$

The fluctuations of the parameter X are accordingly characterized by a structure factor $S_X(\mathbf{q}, \omega) = \frac{9}{R_0^2}S_r(\mathbf{q}, \omega)$. Since the sphere dynamics are uncorrelated, the structure factor is uniform in wave vectors until reaching $q_{\max} \sim \rho_s^{1/3}$, associated with the typical intersphere distance. Hence, we obtain the following structure factor of the internal density of the breathing spheres X:

$$S_X^{\text{breath}}(\mathbf{q}, \omega) \approx \frac{18\gamma k_B T}{mR_0^2}\frac{1}{(\gamma\omega)^2 + \omega_0^4}\frac{(2\pi)^3}{V_q}\theta(q_{\max} - q), \tag{27}$$

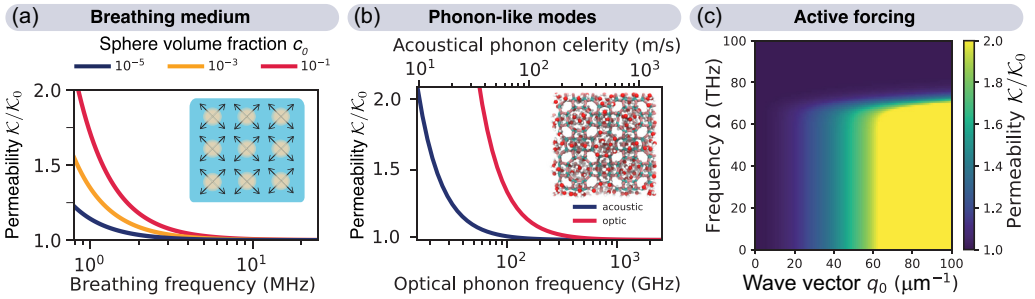

FIG. 2. Fluctuation-induced permeability modification $\mathcal{K}/\mathcal{K}_0$ for various fluctuation spectra S_X of the matrix. (a) Across a breathing medium with sphere volume fraction c_0 as a function of the characteristic frequency $\omega_0/2\pi$. Inset: Schematic of the model. (b) Across a fluctuating porosity with phonon-like modes as a function of the characteristic frequency $\omega_0/2\pi$ for dispersionless optical phonons (bottom axis) and as a function of the sound velocity c for propagating acoustic phonons (top axis). Inset: Molecular dynamics image of water in a zeolite. In (a), (b), the solid fluctuations are thermal with temperature $T = 300$ K. (c) Across an actively forced solid matrix as function of the forcing frequencies Ω and wave vector q_0.

where θ is the Heaviside distribution and $V_q = \frac{4\pi}{3} q_{\max}^3$.

We can then compute analytically the correction to the friction coefficient from Eqs. (17) and (18) as

$$\Delta\xi = \frac{45\rho_s \xi_1^2 k_B T}{2m\omega_0^2 \nu q_{\max}^2 R_0^2}\left[1 - \frac{\arctan(q_{\max}\ell(\omega_0))}{q_{\max}\ell(\omega_0)}\right], \tag{28}$$

where

$$\ell(\omega_0)^2 = \frac{\nu}{\xi_0 + \omega_0^2/\gamma} \tag{29}$$

is a viscous diffusive length. Finally, the renormalized permeability of the system simply rewrites in the case of small fluctuations $\langle r^2\rangle = k_B T/m\omega_0^2$:

$$\frac{\mathcal{K}}{\mathcal{K}_0} \simeq 1 + \frac{45\xi_1^2}{2\xi_0 \nu q_{\max}^2}\frac{\langle r^2\rangle}{R_0^2}\left[1 - \frac{\arctan[q_{\max}\ell(\omega_0)]}{q_{\max}\ell(\omega_0)}\right]. \tag{30}$$

The results for the breathing frequency dependence of the permeability are shown in Fig. 2(a). For $\omega_0 \to 0$, the excess permeability is directly proportional to the root mean square (RMS) of the matrix radius as $\Delta\mathcal{K}/\mathcal{K}_0 \propto \langle r^2\rangle/R_0^2$, recovering the quasistatic result as expected. For large ω_0 such that $q_{\max}\ell(\omega_0) \ll 1$, Eq. (30) reduces to

$$\frac{\mathcal{K}}{\mathcal{K}_0} \simeq 1 + \frac{15\xi_1^2}{2\xi_0^2}\frac{\langle r^2\rangle}{R_0^2}\frac{1}{1 + \omega_0^2/\gamma\xi_0}, \tag{31}$$

which decays like $1/\omega_0^2$. For $\omega_0 \to \infty$, the dynamics of the liquid no longer couples with the hydrodynamics and the permeability enhancement vanishes.

B. Permeability across a fluctuating porosity with phonon-like modes

Beyond the previous simple model, the solid matrix dynamics usually exhibit more complex dynamical features, such as (optical or acoustic) phonons. Acoustic phonons describe propagating waves, while optical phonons are associated with (nearly) dispersionless breathing. Phonon modes are rooted in the dynamics of the displacement field of the porous matrix, say $\mathbf{u}$, and the parameter X is accordingly defined as the normalized density of the matrix as $X = -\nabla\cdot\mathbf{u}$. It is now a time- and space-dependent fluctuating quantity. The fluctuation of the density will affect accordingly the

pore size of the porous medium, hence the Darcy friction. As a rule of thumb, let us consider a dense porous material with a typical pore size R. The fluctuation of the density will therefore affect the pore radius as $R = R_0(1 + \frac{1}{3}X)$. The Darcy friction stems from the viscous flow inside the porosity and should accordingly scale as $\xi \propto 1/R^2$. The friction thus writes $\xi(X) = \xi_0 + \xi_1 X$ with $\xi_1 = -(2/3)\xi_0$ in this case. In a porous material with a more complex structure, coefficients may differ but a similar linear expansion of $\xi(X)$ is expected.

We now turn to the structure factor and first consider acoustic phonons with sound velocity c. We consider a classical phonon description in terms of springs separating atoms of mass m with drag coefficient γ, and the dynamical equation governing the displacement field $\mathbf{u}$ reads in the continuous limit

$$m\partial_t^2\mathbf{u} = -m\gamma\,\partial_t\mathbf{u} + mc^2\nabla^2\mathbf{u} - \nabla V_{\text{ext}}, \tag{32}$$

with V_{ext} an external potential. Hence going to Fourier space, we deduce the response function for X as

$$X(\mathbf{q},\omega) = \frac{1}{m}\frac{q^2}{\omega^2 - q^2c^2 + i\gamma\omega}V_{\text{ext}}(\mathbf{q},\omega), \tag{33}$$

and the fluctuation-dissipation theorem gives

$$S_X^{\text{ph}}(\mathbf{q},\omega) = \frac{2k_BTm}{\omega\rho_m^s}\text{Im}\left(\frac{1}{m}\frac{q^2}{\omega^2 - \omega_q^2 + i\gamma\omega}\right), \tag{34}$$

with $\omega_q = c\,q$ for acoustic phonons and ρ_m^s is the global mass density of the solid. Taking the limit $\gamma \to 0$ leads us to the simplified form for the structure factor associated with phonon-like excitations

$$S_X^{\text{ph}}(\mathbf{q},\omega) = \frac{\pi k_BTq^2}{\rho_m^s\omega^2}\delta(\omega \pm \omega_q). \tag{35}$$

In the following we will assume that the wave vector q is limited by the interatomic distance a, i.e., $q \leqslant q_{\text{max}} = 2\pi/a$. For optical phonons, one finds the same expression except that the dispersion relation is now $\omega_q = \omega_0$, where ω_0 is the constant optical phonon frequency.

In the quasistatic limit, one can deduce the permeability deviation $\Delta\mathcal{K}/\mathcal{K}$ in terms of the RMS of the parameter X. The latter is given by

$$\langle X^2\rangle = \int_0^\infty \text{d}\omega \int_0^{q_{\text{max}}} \text{d}q\, q^2\, S_X^{\text{ph}}(q,\omega). \tag{36}$$

A straightforward analytical evaluation of these integrals leads to the quasistatic estimate for acoustic phonons

$$\mathcal{K} \simeq \mathcal{K}_0\left(1 + \frac{2q_{\text{max}}^3}{27\pi^2\rho_m^s c^2}k_BT\right). \tag{37}$$

Of note, we find a permeability enhancement which scales with $1/c^2$. This is originates in the contribution of lower-energy phonon states which are more populated at a given temperature.

Now beyond the quasistatic regime, Eqs. (17) and (18) allows us to calculate the renormalized permeability $\mathcal{K}/\mathcal{K}_0$ using the full expression for the X spectrum. The results for the permeability as a function of the phonon frequency are shown in Fig. 2(b): the permeability is plotted as a function of the frequency ω_0 for the optical phonons (bottom axis) and as a function of the sound velocity c for the acoustic phonons (top axis). In both cases, we find a strong permeability enhancement for soft solid matrices, associated with low-frequency modes or low sound velocity. While this follows the same trend as in the quasistatic limit, we find important quantitative corrections in the general case due to the dynamical contribution of the overlap between the phonon modes of the matrix and the hydrodynamic modes which do strongly increase the permeability.

C. Permeability across an actively forced solid matrix

Finally, the solid may be subject to an active external forcing at a frequency Ω and (isotropic) spatial wave vector q_0. The effective structure factor of the fluctuations writes accordingly

$$S_X^{\rm act}(\mathbf{q},\omega) = (2\pi)^2 \frac{A}{\rho_s^{2/3}} \delta(\omega-\Omega)\delta(q-q_0), \tag{38}$$

where ρ_s is the solid particle density and A is an dimensionless amplitude of the forcing. The resulting permeability enhancement is shown in Fig. 2(c) for a range of frequencies and wavevectors of the external active forcing [the value $\xi_1 = -(2/3)\xi_0$ was assumed for simplicity]. We observe a permeability enhancement in a broad region of the frequency wave-vector space. The amplification is maximum for large q_0, for which the viscous frequency νq_0^2 dominates over the bare friction ξ_0. In contrast, the effect disappears for large frequency Ω, as the fluid decouples from the forcing. Altogether, it appears possible to enhance the permeability of a porous matrix through an external forcing with well-chosen wavelength and frequency.

V. CONCLUSION

Using perturbation theory of a fluctuating Darcy equation, we have shown that the matrix fluctuations renormalize the fluid permeability as they couple to hydrodynamic modes. In a counterintuitive way, this renormalization effect increases the flow permeability in the models under scrutiny. Our model is minimal in terms of assumption and merely serves as an illustration to show the effect of matrix fluctuations. While corrections to our minimal model may reduce the effect—and perhaps even lead to a permeability reduction in some cases—our results nevertheless reveal that fluctuations of a porous matrix can modulate significantly its permeability to fluid flow and provides insights in the phenomenology and ingredients at play. Indeed, we find that the permeability enhancement is optimal in the case of frequency matching between the modes of the solid and the hydrodynamic fluctuations of the fluid. By exploring elementary models of solid that describe their thermal fluctuations (breathing, phononic), we also provide hints as to the link between the microscopic characteristics of the porous matrix and its hydrodynamic permeability. Furthermore, we show that an external forcing could also be used to control and increase the permeability by exciting well-chosen modes in the solid. For specific systems, numerical molecular dynamics simulations that account for solid fluctuations successfully explored the modulation of ionic diffusion, and could be extended to study mass transport, providing valuable quantitative estimates of permeability modulation.

Beyond our model, it would be interesting to extend such formalism to account for a more general framework of the solid's fluctuations, including coupling to the liquid's volume, correlation with hydrodynamic fluctuations and non-Gaussian correlations. In terms of systems, it would be also interesting to investigate the individual and collective motion of penetrants in fluctuating anisotropic (polymer or glass-forming) matrices [22,37].

Overall, our results provide a new direction of research for nanofluidics and suggest new strategies for improving the efficiency of membranes. Indeed, exploiting membrane fluctuations seems to be a promising and unexplored lever to circumvent the permeability-selectivity trade-off that hinders membrane-based separation technologies.

ACKNOWLEDGMENTS

The authors acknowledge support from ERC project *n-AQUA*, Grant Agreement No. 101071937. B.C. and A.S. acknowledge support from the CFM Foundation. B.C. acknowledges support from the NOMIS Foundation.

DATA AVAILABILITY

No data were created or analyzed in this study.

APPENDIX A: PERTURBATION THEORY FOR THE RENORMALIZED PERMEABILITY AND VISCOSITY

We provide some details of the calculation described in Sec. III B.

As shown in Sec. III B, the self-energy takes the expression

$$\mathbf{\Sigma}(\mathbf{q},\omega) = \xi_1^2 \int \frac{\mathrm{d}\bar{\mathbf{q}}\mathrm{d}\bar{\omega}}{(2\pi)^4} G_{\mathbf{v}}^0(\bar{\mathbf{q}},\bar{\omega}) S_X(\mathbf{q}-\bar{\mathbf{q}},\omega-\bar{\omega}) \mathbf{J}(\mathbf{q})\mathbf{J}(\bar{\mathbf{q}})\mathbf{J}(\mathbf{q}), \tag{A1}$$

where we recall that the projector matrix is defined as $\mathbf{J} = \mathrm{Id} - \mathbf{q}\mathbf{q}/q^2$. Note that we use the identity $\mathbf{J}^2 = \mathbf{J}$. The self-energy is in general a matrix in spatial coordinates.

We can simplify this expression by noting that the self-energy reduces to a multiple of $\mathbf{J}(\mathbf{q})$ for isotropic systems. Indeed, we can define spherical coordinates around the direction of $\mathbf{q}$ and explicit the effect of the self-energy matrix on a generic vector $\mathbf{w} = (w \quad \theta_w \quad 0)_{\mathrm{sph}}$. Here we have fixed φ according to the direction of $\mathbf{w}$. We denote $\bar{\mathbf{q}} = (\bar{q} \quad \bar{\theta} \quad \bar{\varphi})_{\mathrm{sph}}$. Then, in the associated Cartesian coordinates we have

$$\mathbf{J}(\mathbf{q})\mathbf{J}(\bar{\mathbf{q}})\mathbf{J}(\mathbf{q})\mathbf{w} = w\cos(\theta_w) \times (0 \quad 1-\cos(\bar{\theta})^2\cos(\bar{\varphi})^2 \quad -\cos(\bar{\theta})^2\cos(\bar{\varphi})\sin(\bar{\varphi}))_{\mathrm{Cart}}. \tag{A2}$$

Since the system is isotropic, $G_{\mathbf{v}}^0$ and S_X only depend on the norms of $\bar{\mathbf{q}}$ and $\mathbf{q}-\bar{\mathbf{q}}$. In particular, they do not depend on $\bar{\varphi}$. Thus averaging on $\bar{\varphi}$ we obtain

$$\langle \mathbf{J}(\mathbf{q})\mathbf{J}(\bar{\mathbf{q}})\mathbf{J}(\mathbf{q})\mathbf{w}\rangle_{\bar{\varphi}} = w\cos(\theta_w) \times \big(0 \quad 1-\tfrac{1}{2}\cos(\bar{\theta})^2 \quad 0\big)_{\mathrm{Cart}} = \big(1-\tfrac{1}{2}\cos(\bar{\theta})^2\big)\mathbf{J}(\mathbf{q})\mathbf{w}. \tag{A3}$$

Therefore, the projector $\mathbf{J}(\mathbf{q})$ being already present in Eq. (12), we can see the self-energy as a scalar function

$$\Sigma(\mathbf{q},\omega) = \xi_1^2 \int \frac{\mathrm{d}\bar{\mathbf{q}}\mathrm{d}\bar{\omega}}{(2\pi)^4} \left[1 - \frac{1}{2}\left(\frac{\mathbf{q}\cdot\bar{\mathbf{q}}}{q\bar{q}}\right)^2\right] G_{\mathbf{v}}^0(\bar{\mathbf{q}},\bar{\omega}) S_X(\mathbf{q}-\bar{\mathbf{q}},\omega-\bar{\omega}). \tag{A4}$$

Relaxing the incompressibility assumption, we would have a similar result with a more complicated and frequency-dependent additional geometrical factor. Now, for $q \ll \bar{q}$ the isotropic function $S_X(\mathbf{q}-\bar{\mathbf{q}},\omega-\bar{\omega})$ no longer depends on the angle $\mathbf{q}\cdot\bar{\mathbf{q}}$ and the geometrical factor $1-\frac{1}{2}(\frac{\mathbf{q}\cdot\bar{\mathbf{q}}}{q\bar{q}})^2$ reduces to $\frac{5}{6}$ upon integration.

As shown in the main text, the renormalized Green's function of the flow then takes the expression

$$G_{\mathbf{v}}(\mathbf{q},\omega) = \frac{1}{G_{\mathbf{v}}^0(\mathbf{q},\omega)^{-1} - \Sigma(\mathbf{q},\omega)} = \frac{1}{q^2\nu + \xi_0 - \Sigma(\mathbf{q},\omega) - i\omega}. \tag{A5}$$

By isotropy, we can expand the self-energy as a function of q:

$$\Sigma(\mathbf{q},\omega) = \Sigma(q=0,\omega) + \tfrac{1}{2}\partial_q^2\Sigma(q=0,\omega)q^2 + \cdots. \tag{A6}$$

The quadratic term provides the correction to the viscosity at small frequency. Note that the geometrical factor $1-\frac{1}{2}(\frac{\mathbf{q}\cdot\bar{\mathbf{q}}}{q\bar{q}})^2$ depends only on the angle between $\mathbf{q}$ and $\bar{\mathbf{q}}$ but not on the norm q. Thus, we obtain

$$\Delta\xi = \Sigma(0,0) = \frac{5}{6}\xi_1^2 \int_0^\infty \frac{\mathrm{d}q\mathrm{d}\omega}{2\pi^3} q^2 S_X(q,\omega)\mathrm{Re}\big[G_{\mathbf{v}}^0(q,\omega)\big], \tag{A7}$$

$$\Delta\eta = \frac{1}{2}\partial_q^2\Sigma(q=0,0) = \frac{5}{6}\xi_1^2 \int_0^\infty \frac{\mathrm{d}q\mathrm{d}\omega}{4\pi^3} q^2 S_X(q,\omega)\partial_q^2\mathrm{Re}\big[G_{\mathbf{v}}^0(q,\omega)\big]. \tag{A8}$$

The resulting viscosity deviation vanishes for the model of breathing, which happens at $\mathbf{q}=0$, and is small for the other models as shown in Fig. 3.

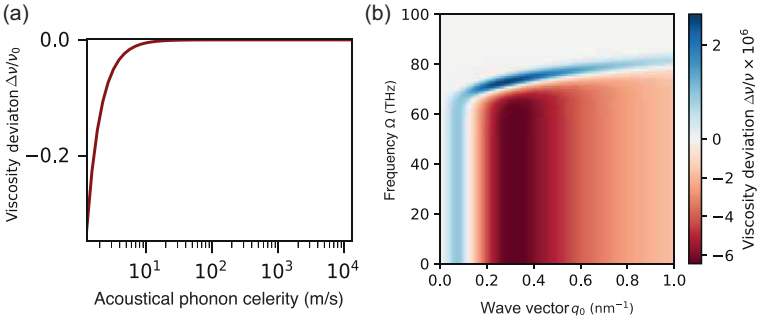

FIG. 3. Fluctuation-induced viscosity deviation $\Delta\nu/\nu_0$ for various fluctuation spectra S_X of the matrix. (a) Across a fluctuating porosity with phonon-like modes as a function of the sound velocity c for propagating acoustic phonons. The solid fluctuations are thermal with temperature $T = 300$ K. (b) Across an actively forced solid matrix as function of the forcing frequencies Ω and wave vector q_0.

APPENDIX B: NUMERICAL COMPUTATIONS

The numerical parameters used to obtain the plots given in the main text are summarized in Table I.

TABLE I. Parameters used in numerical computations.

Liquid	$T = 300$ K
	$\nu = 10^{-6}$ m^2 s^{-1}
	$\rho_m = 10^3$ kg/m^3
Breathing spheres	$R_0 = 1$ nm
	$c = \frac{4}{3}\pi R^3 \rho_s$
	$q_{\max} = \rho_s^{1/3}$
	$\gamma = 10^6$ s^{-1}
	$m = 10^{-14}$ kg
	$\alpha = 1.7601$
	$\eta = 10^{-3}$ Pa s
Phonons	$\xi_0 = 4 \times 10^{10}$ s^{-1}
	$\xi_1 = -\frac{2}{3}\xi_0$
	$\rho_m^s = 2.25 \times 10^3$ kg/m^{-3}
	$q_{\max} = 2\pi/a$, $a = 1$ Å
Forcing	$\rho_s = 10^{18}$ m^{-3}
	$A = 10^{-3}$

[1] H. B. Park, J. Kamcev, L. M. Robeson, M. Elimelech, and B. D. Freeman, Maximizing the right stuff: The trade-off between membrane permeability and selectivity, Science **356**, eaab0530 (2017).
[2] J. R. Werber, C. O. Osuji, and M. Elimelech, Materials for next-generation desalination and water purification membranes, Nat. Rev. Mater. **1**, 16018 (2016).
[3] Y. Gogotsi and B. Anasori, The rise of MXenes, ACS Nano **13**, 8491 (2019).
[4] A. Siria, M.-L. Bocquet, and L. Bocquet, New avenues for the large-scale harvesting of blue energy, Nat. Rev. Chem. **1**, 0091 (2017).
[5] S. Faucher, N. Aluru, M. Z. Bazant, D. Blankschtein, A. H. Brozena, J. Cumings, J. Pedro de Souza, M. Elimelech, R. Epsztein, J. T. Fourkas *et al.*, Critical knowledge gaps in mass transport through single-digit nanopores: A review and perspective, J. Phys. Chem. C **123**, 21309 (2019).
[6] S. Marbach and L. Bocquet, Osmosis, from molecular insights to large-scale applications, Chem. Soc. Rev. **48**, 3102 (2019).
[7] L. Bocquet, Nanofluidics coming of age, Nat. Mater. **19**, 254 (2020).
[8] P. Robin and L. Bocquet, Nanofluidics at the crossroads, J. Chem. Phys. **158**, 160901 (2023).
[9] N. R. Aluru, F. Aydin, M. Z. Bazant, D. Blankschtein, A. H. Brozena, J. P. de Souza, M. Elimelech, S. Faucher, J. T. Fourkas, V. B. Koman *et al.*, Fluids and electrolytes under confinement in single-digit nanopores, Chem. Rev. **123**, 2737 (2023).
[10] L. Bocquet and E. Charlaix, Nanofluidics, from bulk to interfaces, Chem. Soc. Rev. **39**, 1073 (2010).
[11] B. Davidovitch, E. Moro, and H. A. Stone, Spreading of viscous fluid drops on a solid substrate assisted by thermal fluctuations, Phys. Rev. Lett. **95**, 244505 (2005).
[12] R. Fetzer, M. Rauscher, R. Seemann, K. Jacobs, and K. Mecke, Thermal noise influences fluid flow in thin films during spinodal dewetting, Phys. Rev. Lett. **99**, 114503 (2007).
[13] F. C. Detcheverry and L. Bocquet, Thermal fluctuations in nanofluidic transport, Phys. Rev. Lett. **109**, 024501 (2012).
[14] S. Y. Noskov, S. Berneche, and B. Roux, Control of ion selectivity in potassium channels by electrostatic and dynamic properties of carbonyl ligands, Nature (London) **431**, 830 (2004).
[15] G. Bhabha, J. Lee, D. C. Ekiert, J. Gam, I. A. Wilson, H. J. Dyson, S. J. Benkovic, and P. E. Wright, A dynamic knockout reveals that conformational fluctuations influence the chemical step of enzyme catalysis, Science **332**, 234 (2011).
[16] G. Wei, W. Xi, R. Nussinov, and B. Ma, Protein ensembles: How does nature harness thermodynamic fluctuations for life? The diverse functional roles of conformational ensembles in the cell, Chem. Rev. **116**, 6516 (2016).
[17] R. Zwanzig, Dynamical disorder: Passage through a fluctuating bottleneck, J. Chem. Phys. **97**, 3587 (1992).
[18] M. Ma, F. Grey, L. Shen, M. Urbakh, S. Wu, J. Z. Liu, Y. Liu, and Q. Zheng, Water transport inside carbon nanotubes mediated by phonon-induced oscillating friction, Nat. Nanotechnol. **10**, 692 (2015).
[19] M. Ma, G. Tocci, A. Michaelides, and G. Aeppli, Fast diffusion of water nanodroplets on graphene, Nat. Mater. **15**, 66 (2016).
[20] E. R. Cruz-Chú, E. Papadopoulou, J. H. Walther, A. Popadić, G. Li, M. Praprotnik, and P. Koumoutsakos, On phonons and water flow enhancement in carbon nanotubes, Nat. Nanotechnol. **12**, 1106 (2017).
[21] S. Marbach, D. S. Dean, and L. Bocquet, Transport and dispersion across wiggling nanopores, Nat. Phys. **14**, 1108 (2018).
[22] M. Kanduc, W. K. Kim, R. Roa, and J. Dzubiella, Selective molecular transport in thermoresponsive polymer membranes: Role of nanoscale hydration and fluctuations, Macromolecules **51**, 4853 (2018).
[23] Y. Noh and N. Aluru, Phonon-fluid coupling enhanced water desalination in flexible two-dimensional porous membranes, Nano Lett. **22**, 419 (2021).
[24] A. Schlaich, M. Vandamme, M. Plazanet, and B. Coasne, Bridging microscopic dynamics and hydraulic permeability in mechanically-deformed nanoporous materials, ACS Nano **18**, 26011 (2024).
[25] N. Ferreira de Souza, C. Picard, L. F. M. Franco, and B. Coasne, Thermal conductivity of a fluid-filled nanoporous material: Underlying molecular mechanisms and the rattle effect, J. Phys. Chem. B **128**, 2516 (2024).

[26] Z. Waysenson, A. France-Lanord, A. Serva, P. Simon, M. Salanne, and A. M. Saitta, Electrode flexibility enhances electrolyte dynamics during supercapacitor charging, ACS Nano **1**9, 29462 (2025).
[27] N. Kavokine, M.-L. Bocquet, and L. Bocquet, Fluctuation-induced quantum friction in nanoscale water flows, Nature (London) **602**, 84 (2022).
[28] A. T. Bui, F. L. Thiemann, A. Michaelides, and S. J. Cox, Classical quantum friction at water–carbon interfaces, Nano Lett. **23**, 580 (2023).
[29] B. Coquinot, M. Becker, R. R. Netz, L. Bocquet, and N. Kavokine, Collective modes and quantum effects in two-dimensional nanofluidic channels, Faraday Discuss. **249**, 162 (2024).
[30] M. Lizée, B. Coquinot, G. Mariette, A. Siria, and L. Bocquet, Anomalous friction of supercooled glycerol on mica, Nat. Commun. **15**, 6129 (2024).
[31] B. Coquinot, L. Bocquet, and N. Kavokine, Quantum feedback at the solid-liquid interface: Flow-Induced electronic current and its negative contribution to friction, Phys. Rev. X **13**, 011019 (2023).
[32] B. Coquinot, L. Bocquet, and N. Kavokine, Hydroelectric energy conversion of waste flows through hydroelectronic drag, Proc. Natl. Acad. Sci. USA **121**, e2411613121 (2024).
[33] B. Coquinot, A. T. Bui, D. Toquer, A. Michaelides, N. Kavokine, S. J. Cox, and L. Bocquet, Momentum tunneling between nanoscale liquid flows, Nat. Nanotechnol. **20**, 397 (2025).
[34] K. Falk, B. Coasne, R. Pellenq, F.-J. Ulm, and L. Bocquet, Subcontinuum mass transport of condensed hydrocarbons in nanoporous media, Nat. Commun. **6**, 6949 (2015).
[35] J. Bear, *Modeling Phenomena of Fllow and Transport in Porous Media*, Theory and Applications of Transport in Porous Media, Vol. 31 (Springer International, Cham, Switzerland, 2018).
[36] A. S. Sangani and A. Acrivos, Slow flow through a periodic array of spheres, Int. J. Multiphase Flow **8**, 343 (1982).
[37] R. Zhang and K. S. Schweizer, Correlated matrix-fluctuation-mediated activated transport of dilute penetrants in glass-forming liquids and suspensions, J. Chem. Phys. **146**, 194906 (2017).